Regenerative Therapy 23 (2023) 44–51

Contents lists available at ScienceDirect

Regenerative Therapy

journal homepage: http://www.elsevier.com/locate/reth

Original Article

Modified gelatin hydrogel nonwoven fabrics (Genocel) as a skin substitute in murine skin defects

Yuanjiaozi Li [a], Michiharu Sakamoto [a, *], Kumiko Matsuno [b, c], Eiichi Sawaragi [a], Qiannan Zhao [a], Takashi Nakano [a], Hiroki Yamanaka [a], Itaru Tsuge [a], Yasuhiro Katayama [a], Naoki Shimada [c], Yuuka Watahiki [c], Yasuhiko Tabata [b], Naoki Morimoto [a]

[a] Department of Plastic and Reconstructive Surgery, Graduate School of Medicine, Kyoto University, Sakyo-ku, Kyoto, Japan
[b] Laboratory of Biomaterials, Institute for Frontier Life and Medical Sciences, Kyoto University, Sakyo-ku, Kyoto, Japan
[c] Research and Development Center, The Japan Wool Textile Co., Ltd., Kakogawa, Hyogo, Japan

ARTICLE INFO

Article history:
Received 19 February 2023
Accepted 21 March 2023

Keywords:
Skin substitute
Water content
Degradation
Wound healing
Gelatin hydrogel
Skin defects

ABSTRACT

Introduction: From previous research, an emerging material composed of gelatin hydrogel nonwoven fabric (Genocel) has shown potential as a skin substitute, by improving neovascularization promotion in the early phase of wound healing. However, Genocel was inferior in terms of granulation formation compared to Pelnac. To solve this problem, we modified the manufacturing process of Genocel to reduce its water content, extend the degradation time (Genocel-L), and evaluate its healing process as a skin substitute.

Methods: Genocel with a low water content (Genocel-L) was prepared and the difference in water content compared to that of the conventional Genocel was confirmed. Degradation tests were performed using collagenase and compared among Genocel-L, Genocel, and Pelnac sheets. In the in vivo study, sheets of Genocel-L or Pelnac were applied to skin defects created on the backs of C57BL/6JJcl mice. On days 7, 14, and 21, the remaining wound area was evaluated and specimens were harvested for Hematoxylin and Eosin, Azan, anti-CD31, CD68, and CD163 staining to assess neoepithelialization, granulation tissue, capillary formation, and macrophage infiltration.

Results: Genocel-L had a lower water content than the conventional Genocel and a slower degradation than Genocel and Pelnac. In the in vivo experiment, no significant differences were observed between Genocel-L and Pelnac in relation to the wound area, neoepithelium length, granulation formation, and the number of newly formed capillaries. The area of newly formed capillaries in the Pelnac group was significantly larger than that in the Genocel-L group on day 21 ($p < 0.05$). Regarding macrophage infiltration, significantly more M2 macrophages were induced in the Pelnac group on days 14 and 21, and the M2 ratio was larger in the Pelnac group ($p < 0.05$) during the entire process.

Conclusions: Genocel-L has a lower water content and slower degradation rate than the conventional Genocel. Genocel-L had equivalent efficacy as a skin substitute to Pelnac, and can therefore be considered feasible for use as a skin substitute. However, a manufacturing method that can further modify Genocel-L is required to recover its early angiogenic potential.

1. Introduction

The fundamental role of the skin is to provide a supportive barrier to protect the body against harmful agents and injuries. Skin defects resulting from trauma or tumor resection not only allow for bacterial invasion from the external environment but also result in body fluid loss. Skin substitutes are widely used to temporarily provide a barrier between the external environment and the internal environment of the body [1–3]. The numerous skin substitutes available can be divided into epidermal, dermal, and dermoepidermal based on their components, as well as autologous, allogeneic, and xenogeneic based on their origin [4]. Characteristics such as stability, cytocompatibility, angiogenic properties, and low antigenicity are required for materials to be used as skin substitutes [5,6].

* Corresponding author. 54 Kawahara-cho Shogoin, Sakyo-ku, Kyoto, 606-8507, Japan.
E-mail address: dojis@kuhp.kyoto-u.ac.jp (M. Sakamoto).
Peer review under responsibility of the Japanese Society for Regenerative Medicine.

https://doi.org/10.1016/j.reth.2023.03.003

We previously reported on the potential of Genocel (NIKKE MEDICAL Co., Ltd., Osaka, Japan), a commercially available scaffold for three-dimensional cell culture, as a new skin substitute [7]. Genocel, gelatin hydrogel nonwoven fabrics [8–11], is produced by a solution blow method using gelatin solution [8,12], which demonstrates the high mechanical strength needed to maintain a porous structure enabling cells to infiltrate and distribute homogeneously [9,11]. When Genocel was applied to skin defects in mice, it showed advantages in capillary formation but failed in granulation tissue formation and macrophage infiltration compared to the conventional skin substitute Pelnac [7]. This inferiority could be attributed to the rapid degradation of Genocel, because it was not originally developed for use as a skin substitute. Therefore, we modified the manufacturing process of Genocel to lower its water content and optimize its degradation properties as a skin substitute. In this study, we confirmed the water content and degradation time of the newly prepared materials and compared them with those of Pelnac. The healing process after application was evaluated in murine skin defect models.

2. Materials and methods

Genocel sheets with a diameter of 5 mm were supplied by NIKKE MEDICAL Co., Ltd. (Osaka, Japan). In addition, Genocel with a low water content (Genocel-L) was produced with the same composition and raw materials but with different cross-linking degree. In this study, we used a single-layer Pelnac without an outer silicon layer as a conventional skin substitute.

2.1. Evaluation of the water content of Genocel-L and Genocel

The water content was quantified to clarify the difference between the newly prepared Genocel-L and conventional Genocel. Ten sheets each of dry Genocel-L and Genocel were weighed, and then the sheets were soaked in phosphate buffered saline (PBS) and incubated at 37 °C for 24 h. The sheets were weighed again after removing excess water with paper (Kimtowel; Nippon Paper Crecia Co., Ltd. Tokyo, Japan). Through this process, the gelatin fibers were sufficiently hydrated, and the excess water present between the fibers was removed. Water content was calculated from the ratio of the weight before and after.

2.2. In vitro degradation test of Genocel-L, Genocel and Pelnac

Six sheets each of Genocel-L, Genocel, and Pelnac were prepared. Each sheet was cut to a weight of 2 ± 0.2 mg, using scissors. PBS containing 100 mg/mL $CaCl_2$ and 46.8 mg/mL $MgCl_2$ was prepared, and collagenase solution was prepared by dissolving collagenase D (Roche, Basel, Switzerland) in PBS (50 μg/mL).

Each sheet of Genocel-L, Genocel, or Pelnac was kept in PBS at 37 °C for 24 h in a 1.5 mL centrifuge tube then, PBS was replaced with 1 mL of collagenase solution. At each time point (0.5, 1, 1.5, 2, 2.5, 3, 3.5, 4, 5, 6, 7, and 8 h), the supernatants were collected and replaced with 1 mL of a new collagenase solution until the material was completely degraded. The amount of degraded gelatin contained in the collected solution was measured using the bicinchoninic acid assay kit (code:23,225, Thermo Fisher Scientific Inc.) Precisely, 25 μL each of the samples and bovine serum albumin standard was dispensed into a 96-well plate (code:8404, Thermo Fisher Scientific Inc.). Subsequently, 200 μL of the working reagent was added and mixed thoroughly. After incubation at 37 °C for 30 min, the absorbance was measured at 562 nm using a plate reader (SYNERGY H1, BioTek Vermont, U.S.).

The percentage of remaining material was calculated using Eq. (1):

$$Remaining\ material\ \% = \left(1 - \frac{\sum_{t=0.5}^{n} A_t}{\sum_{t=0.5}^{T} A_t}\right) \times 100\ \% \quad (1)$$

Where A_t is the absorbance at time point t, T is the time for complete degradation, and n is a certain time point (0.5, 1, 1.5, 2, 2.5, 3, 3.5, 4, 5, 6, 7, or 8 h).

2.3. Scanning electron microscopy (SEM)

Dried samples were fixed with a conductive tape, and then coated with sputtered gold using a sputter-coater (MSP-1S; Vacuum Device Inc., Japan). The specimens were observed with a scanning electron microscope (SEM, FlexSEM 1000, Hitachi High Technologies corp., Japan).

2.4. Preparation of Genocel-L and Pelnac sheets for murine experiments

Pelnac sheets 8 mm in diameter were prepared using an 8-mm biopsy punch (Kai Industries Co., Ltd., Japan). Then, Genocel-L and Pelnac sheets were immersed in saline solution (Otsuka Pharmaceutical Factory, Inc., Tokushima, Japan) for over 30 min at room temperature before application. Regarding the size of Genocel-L sheets, a sheet with a diameter of 5 mm reached approximately 8 mm in diameter after immersion in saline solution.

2.5. Application of Genocel-L and Pelnac on skin defects in mice

The animal study was conducted at Kyoto University, following the Guidelines for Animal Experimentation of Kyoto University, Japan (permit number: Med Kyo 20515), and the number of experimental animals used was kept to a minimum. Forty-two C57BL/6JJcl mice (male, 8–9 weeks old) (CLEA Japan, Inc., Tokyo, Japan) were fed and housed individually per cage in a temperature-controlled animal facility with a 12-h light/dark cycle. One day before the surgical procedure, the hair on the back of each mouse was shaved using an electric shaver (Thrive; Daito Electric Machine Ind. Co., Ltd., Osaka, Japan) and depilated using depilation cream (Kracie, Tokyo, Japan).

The mice were separated into two groups: Genocel-L and Pelnac. After the application of Genocel-L or Pelnac to the wounds, the healing process was evaluated using a previously established murine skin defect model [7]. Briefly, a donut-shaped silicone skin splint (18/12 mm in outer/inner diameter) was attached and sutured to the skin on the back of the mice, using 5–0 nylon, to prevent wound contraction. Subsequently, a full-thickness skin defect, 8 mm in diameter, at the center of the applied skin splint was created, and a Genocel-L or Pelnac sheet was applied to the skin defect. The wound was then covered with a silicone mesh sheet (9 mm in diameter; SI-mesh, Alcare, Japan), fixed to the marginal skin by suturing, covered with gauze, and secured with a surgical tape bandage to prevent contamination and mechanical stress. All painful procedures were performed under general anesthesia with isoflurane (Pfizer Inc., Tokyo, Japan) in spontaneously breathing animals. The concentration of isoflurane was kept at 1.5–2% to provide an appropriate depth of anesthesia. After these procedures, the mice were placed in individual cages inside the institutional animal facility.

2.6. Tissue harvesting and sample preparation

The wounds were evaluated and harvested 7, 14, and 21 days after surgery. Seven mice were euthanized by carbon dioxide gas inhalation at each time point in each group, and the wounds were photographed with a digital camera (Sony Corporation, Tokyo, Japan). The wound specimens, including surrounding tissue, were harvested, fixed in 10% formalin buffer solution (FUJIFILM Wako Pure Chemical Co., Ltd., Osaka, Japan), paraffin embedded, and sectioned at the center of each wound, axially. Hematoxylin and eosin (HE) staining, Azan staining, and immunohistochemical staining for CD31, CD163, and CD68 antibodies were performed.

CD31 is a specific marker for endothelial cells [13], which is used to detect capillaries in sections. For anti-CD31 staining, the sections were deparaffinized and rehydrated, and heat-induced antigen retrieval was performed in ethylenediaminetetraacetic acid (EDTA) (Nichirei Biosciences Inc., Tokyo, Japan) at 98 °C for 20 min. Rabbit monoclonal antibody (code: ab182981, Abcam plc., Cambridge, UK) at a 1:10,000 dilution was applied to the sections and incubated at 4 °C overnight. Then, a polymer reagent (simple stain mouse MAX PO; Nichirei Biosciences Inc., Tokyo, Japan) was used as a secondary antibody, and the sections were exposed to DAB (3–3′-diaminobenzidine-4HCl) (Nichirei Biosciences Inc. Tokyo, Japan) and counterstained with hematoxylin.

CD163 is a specific marker for M2 macrophages and CD68 is a pan-macrophage marker [14,15]; therefore, we used anti-CD163 and anti-CD68 stained sections to count the number of M2 macrophages and pan-macrophages, and the M2 ratio was calculated as the ratio of the number of CD163 positive cells to that of CD68 positive cells [15]. For anti-CD68 or CD163 staining, the staining method followed the process of anti-CD31 staining mentioned previously, and rabbit polyclonal antibodies (code: ab125212 and ab182422, respectively, Abcam plc.) were used at different dilutions (1:5000; 1:4000, respectively) instead.

After staining, histological photomicrographs were obtained and analyzed using a BZ-X800 Analyzer (Keyence Corp., Osaka, Japan).

2.7. Evaluation of the remaining wound area

The wound areas were measured on days 7, 14, and 21 by tracing the wound edge on gross photographs using ImageJ software (National Institutes of Health, Bethesda, MD, USA). The remaining wound area was compared between the Genocel-L and Pelnac groups at each time-point.

2.8. Evaluation of neoepithelialization and newly formed granulation tissue

The neoepithelium lengths on days 7 and 14 were evaluated on HE-stained sections by measuring both edges of the wound by tracing the lines from the nearest hair follicle to the end of the epithelium, and the total value was calculated.

Areas of newly formed granulation tissue, generated above the muscle layer, were measured on the Azan-stained sections on days 7, 14, and 21. The fibrous connective tissue in granulation stained light blue with aniline blue; therefore, it was distinguished from the dermis of the wound edge, which stained dark blue. The area of the epidermis that developed over dermis-like tissue was excluded.

2.9. Evaluation of newly formed capillaries and the capillary area

The numbers and total areas of newly formed capillaries were measured in the sections immunochemically stained with anti-CD31 antibody on days 7, 14, and 21. Newly formed capillaries were detected in the area of newly formed granulation tissue, which was determined on Azan-stained sections. According to previous research [16–18], a threshold was set for the brown tint stained with DAB, and spots with a color density higher than this

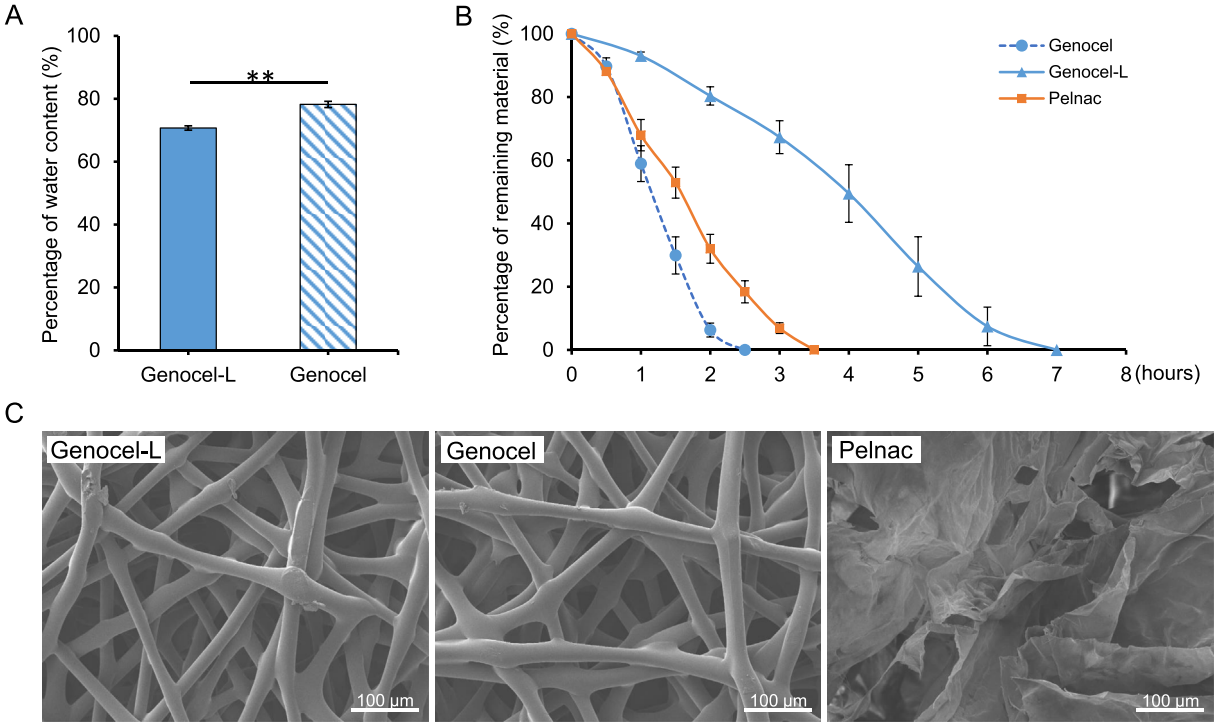

Fig. 1. Analysis of in vitro characteristics of materials. A. Comparison of the water content between Genocel-L and Genocel. **p < 0.01. B. Comparison of the degradation time among Genocel-L, Genocel and Pelnac. C. SEM images of Genocel-L, Genocel and Pelnac. Scale bar: 100 μm.

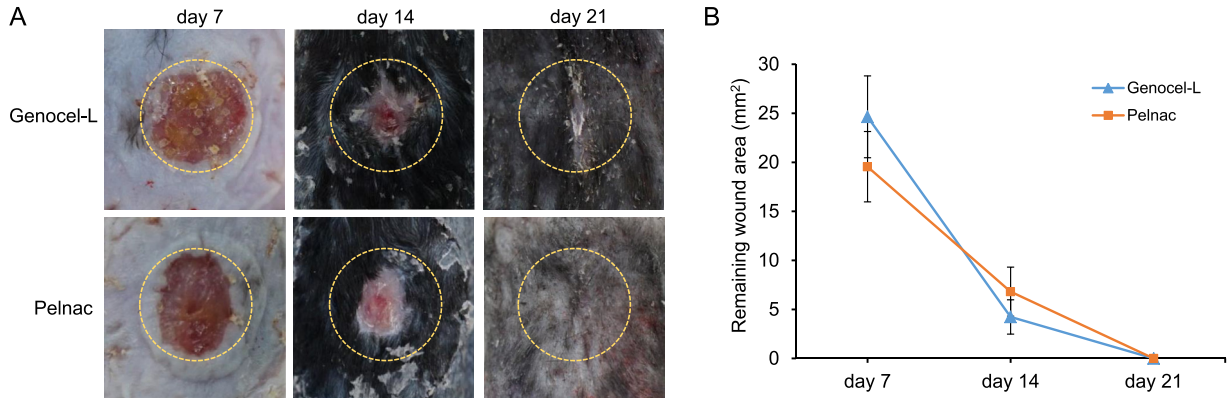

Fig. 2. Assessment of remaining wound area. A. Macroscopic views of the wound after sheets of Genocel-L or Pelnac were applied to the skin defects created on mice, observed on days 7, 14, and 21. Diameter of the round scale: 8 mm. B. Comparison of the remaining wound area on days 7, 14 and 21. No significant difference was detected.

threshold were counted as capillaries. The number and area of the capillaries were recorded and calculated using a BZ-X800 Analyzer (Keyence Corp., Osaka, Japan).

2.10. Evaluation of macrophage infiltration

Anti-CD163-stained or anti-CD68-stained sections were used to evaluate the number of M2 macrophages and pan-macrophages on days 7, 14, and 21. The number of M2 macrophages and pan-macrophages was counted in the area of newly formed granulation tissue that was determined on Azan-stained sections and counted using the BZ-X800 Analyzer (Keyence Corp., Osaka, Japan) in a similar way to the capillary measurement, and the M2 ratio was calculated.

2.11. Statistical analysis

All data are presented as the mean ± standard deviation. T-test was used to analyze the data using Microsoft Excel (Microsoft Corp.,

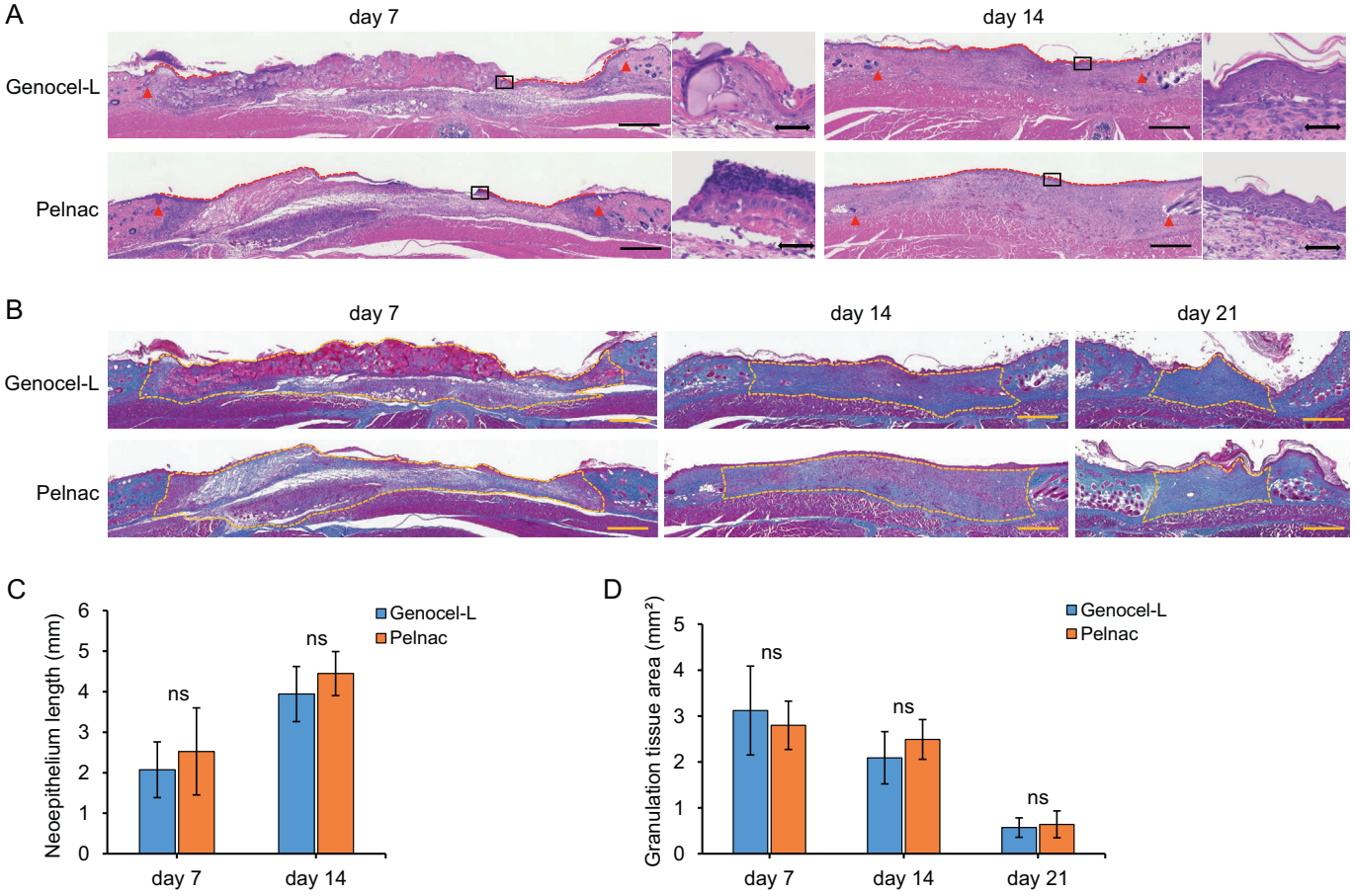

Fig. 3. Assessment of neoepithelium length and newly formed granulation tissue. A. Micrographs of HE-stained sections on days 7 and 14. The neoepithelium length was measured between the end of epithelium and hair follicles in the wound edge. The broken line indicates the neoepithelium. The red arrowhead indicates the nearest hair follicle. Scale bar: 500 μm. Higher magnification scale bar: 50 μm. B. Micrographs of Azan-stained sections on days 7, 14, and 21. The broken lines indicate the newly formed granulation tissue. Scale bar: 500 μm. C. Comparison of the neoepithelium length on days 7 and 14. ns: not significant. D. Comparison of the area of formed granulation on days 7, 14, and 21. ns: not significant.

Redmond, WA, USA). Statistical significance was indicated by probability (P) values < 0.05.

3. Results

3.1. The water content of Genocel-L and Genocel

The water content percentage of Genocel-L was 70.7 ± 0.7%, which was significantly lower than the percentage of 78.2 ± 1.0% observed in the conventional Genocel (Fig. 1A). This confirmed that the water content was modified as expected.

3.2. In vitro degradation time of Genocel-L, Genocel and Pelnac

The complete degradation times of the Genocel-L, Genocel and Pelnac sheets were 7, 2.5, and 3.5 h, respectively. Compared to Genocel and Pelnac, Genocel-L required the longest time for complete degradation in collagenase solution (Fig. 1B). This indicates that the newly prepared Genocel-L was more resistant to enzymatic degradation and could maintain its morphology for a longer period of time.

3.3. SEM of Genocel-L, Genocel and Pelnac

SEM images showed that dried Genocel-L and Genocel contain almost the same network structures with fiber cross-over or fusion at the intersection. In the case of Pelnac, amorphous porous structures were observed (Fig. 1C).

3.4. Assessment of the remaining wound area

The wounds in the Genocel-L and Pelnac groups on days 7, 14, and 21 are shown in Fig. 2A. The time course of the wound area is shown in Fig. 2B. In both groups, the wounds healed completely within 21 days. No significant differences were observed between the two groups during the entire process.

3.5. Assessment of neoepithelium length and granulation tissue

Micrographs of HE-stained sections in the Genocel-L and Pelnac groups on days 7 and 14 are shown in Fig. 3A. Neoepithelium lengths were similar in the Genocel-L and Pelnac groups, and no significant difference was observed (Fig. 3C).

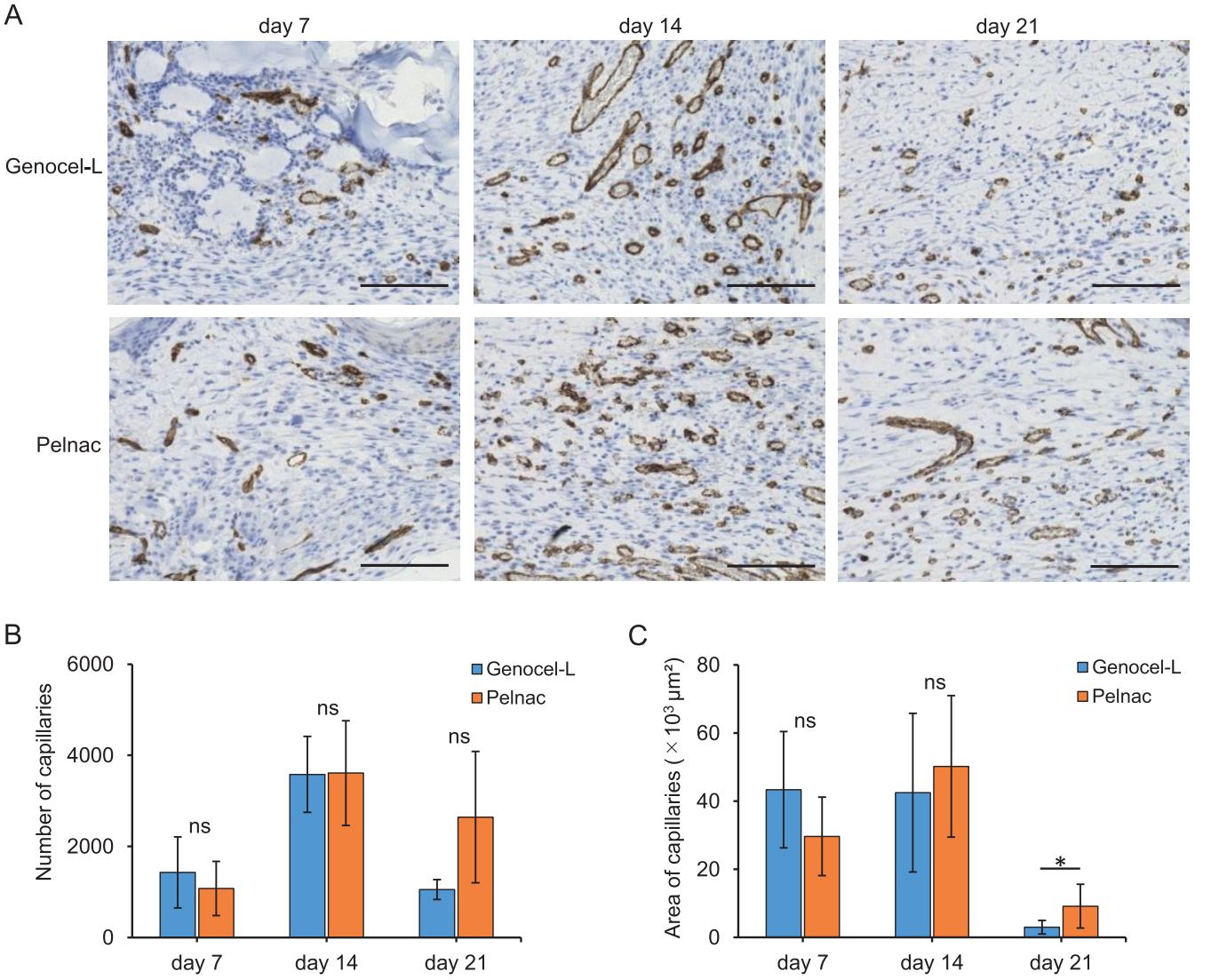

Fig. 4. Assessment of newly formed capillaries. A. Micrographs of anti-CD31-stained sections on days 7, 14, and 21. Scale bar: 100 μm. B. Comparison of the number of newly formed capillaries on days 7, 14, and 21. C. Comparison of the area of newly formed capillaries on days 7, 14, and 21. *p < 0.05. ns: not significant.

Areas of the newly formed granulation tissue were evaluated using Azan-stained sections (Fig. 3B). No significant differences were observed between the Genocel-L and Pelnac groups during the entire process (Fig. 3D). This result indicates that their abilities to promote granulation tissues are equivalent.

3.6. Assessment of newly formed capillaries and capillary area

Micrographs of immunostained sections with anti-CD31 antibody are shown in Fig. 4A.

A significant difference was observed only in the capillary area on day 21: the area of newly formed capillaries in the Pelnac group was significantly larger than that in the Genocel-L group ($p < 0.05$) (Fig. 4C), whereas the number of capillaries was equivalent in both groups during the entire process (Fig. 4B).

3.7. Assessment of macrophage infiltration

The positive cells in the micrographs of sections immunostained with anti-CD 163 or 68 antibodies were counted to evaluate M2-and pan-macrophages, respectively (Fig. 5A and B). The number of pan-macrophages in the Genocel-L group was significantly larger than that in the Pelnac group on day 7 ($p < 0.05$) (Fig. 5D). In contrast, the number of M2 macrophages in the Pelnac group was significantly larger than that in the Genocel-L group on days 14 and 21 ($p < 0.05$) (Fig. 5C). The M2 ratio in the Pelnac group was significantly higher than that in the Genocel-L group during the entire process ($p < 0.05$) (Fig. 5E).

4. Discussion

In this study, we modified the manufacturing method of Genocel by adjusting the water content and reducing the degradation rate to produce Genocel-L. We investigated its properties as a skin substitute. In vivo experiments, Genocel-L was as efficient as the traditional skin substitute Pelnac in terms of wound area reduction, epithelialization, and granulation tissue formation. However, Pelnac was superior in terms of capillary formation on day 21 and M2 macrophage induction.

In our previous report, the conventional Genocel demonstrated an advantage of faster neovascularization compared to Pelnac but revealed its inferiority in inducing granulation tissue formation. To ensure effective granulation tissue formation, it is imperative that the pore inside the material is maintained and its structure as a scaffold is preserved for a substantial duration of time [7,19]. Genocel is composed of a gelatin-based structure optimized not for use as a skin substitute, but for cell culture [9–11]; therefore, it was unable to maintain its structure long enough for granulation tissue to form in vivo. To be used as a skin substitute, the degradation rate of Genocel needed to be optimized.

The in vivo degradability of gelatin hydrogels depends on their water content [20,21]. Therefore, we manufactured Genocel-L with a slower degradation rate by decreasing the water content of the conventional Genocel. As a result, in the murine experiment, Genocel-L showed an equivalent property to induce granulation tissue formation as Pelnac, as expected. On the other hand, Genocel-L lost the advantage of neovascularization that the conventional Genocel had.

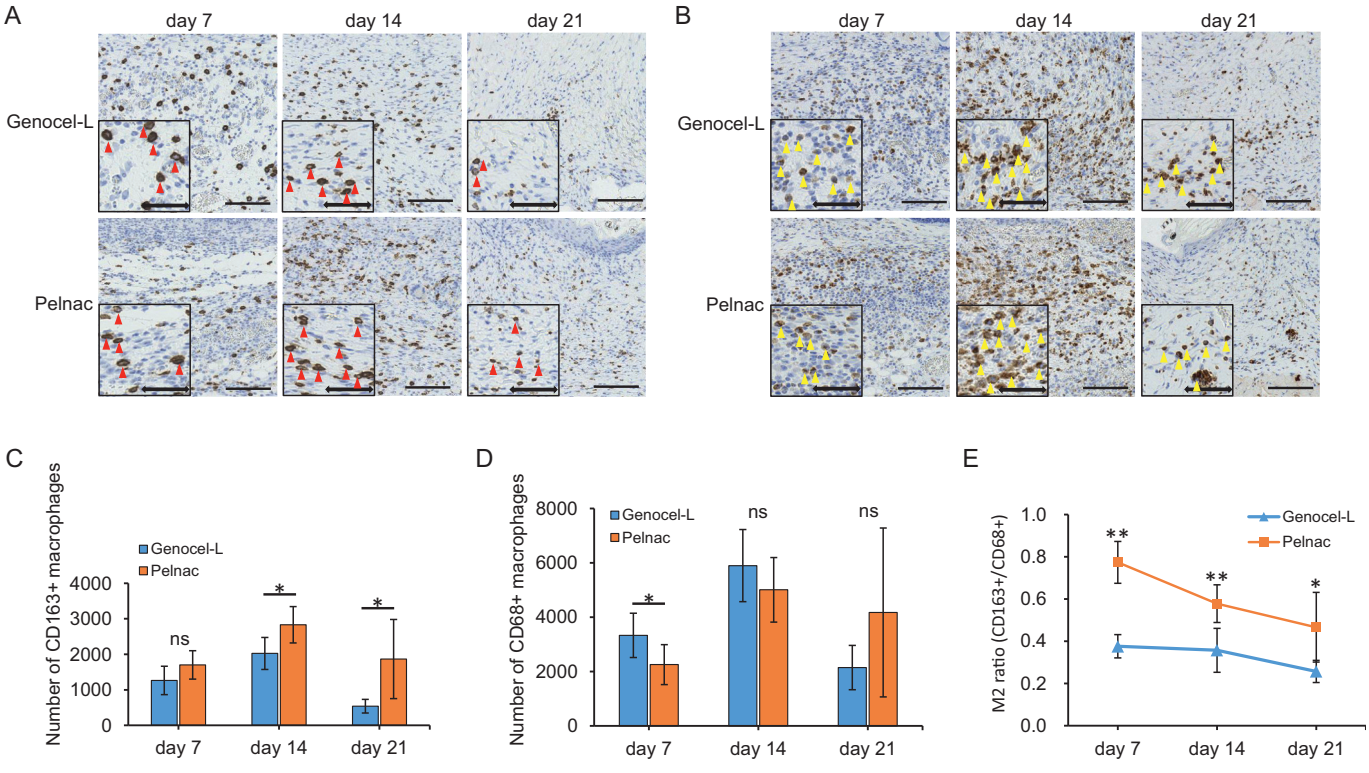

Fig. 5. Assessment of macrophage infiltration. A. Micrographs of anti-CD163-stained sections on days 7, 14, and 21. Scale bar: 100 μm. Higher magnification scale bar: 50 μm. The red arrow heads indicate CD163+ macrophage. B. Micrographs of anti-CD68-stained sections on days 7, 14, and 21. Scale bar: 100 μm. Higher magnification scale bar: 50 μm. The yellow arrow heads indicate $CD68^+$ macrophage. C. Comparison of the number of CD163+ macrophages on days 7, 14, and 21. *$p < 0.05$. ns: not significant. D. Comparison of the number of $CD68^+$ macrophages on days 7, 14, and 21. *$p < 0.05$. ns: not significant. E. Comparison of the M2 ratio (CD163+/CD68+) on days 7, 14, and 21. *$p < 0.05$. **$p < 0.01$.

When applied in vivo, collagen sponges or gelatin hydrogel fabrics are gradually degraded and absorbed to be replaced by the recipient extracellular matrix along with an inflammatory response [22]. Genocel-L maintained its structure longer in vivo than the conventional Genocel, which might provide the environment necessary for fibroblasts to proliferate and migrate. On the other hand, changes in cross-linking degree might have affected not only water content and degradability but also bulk density of the material [23,24], which may be the reason for the lost early angiogenesis advantage of Genocel-L. In particular, compromised degradability may have prevented vascular maturation on day 21.

Macrophages also play an important role in wound healing [25,26]. Macrophages regulate wound healing phases through the transition in macrophage phenotype from the inflammatory phase to the proliferative phase [27–30]. M1 macrophages initiate and sustain inflammatory responses, which mainly mediate the tissue-destructive phase. In contrast, M2 macrophages mainly exert anti-inflammatory effects, which are responsible for the tissue-reparative phase. In this study, Genocel-L had a lower M2 macrophage ratio than Pelnac throughout the observation period. The prolonged degradation of Genocel-L may have retarded the transition from the inflammatory phase to the proliferative and remodeling phases.

However, the physical properties of Genocel and Genocel-L have not yet been studied in detail. A detailed comparison of the effects of each physical factor, such as viscoelasticity, fiber thickness, and pore size, on angiogenesis and macrophage induction is required. Thus, it is necessary to find a manufacturing method that can further modify Genocel-L to recover its early angiogenic potential, while maintaining its ability to form granulation tissue.

We expect Genocel-L to be a novel option for the clinical wound treatment.

5. Conclusions

We prepared a prototype of a modified Genocel (Genocel-L) in which the water content and degradation rate were reduced by modifying the cross-linking conditions. Genocel-L had equivalent efficacy as a skin substitute to Pelnac in terms of wound area reduction, epithelialization, and granulation tissue formation. However, Pelnac was superior in terms of M2 macrophage induction. Genocel-L is considered feasible for use as a skin substitute; however, it still needs to be modified for better angiogenesis.

Declaration of competing interest

All authors declare no conflicts of interest in association with the present study.

Acknowledgements

This research was supported by the Translational Research Network Program (Seeds A) of the Japan Agency for Medical Research and Development (AMED) under grant number JP21lm0203006 and the Japan Wool Textile Co., Ltd. Yuanjiaozi Li was supported by JST SPRING under the grant number JPMJSP2110.

References

[1] Sheikholeslam M, Wright MEE, Jeschke MG, Amini-Nik S. Biomaterials for skin substitutes. Adv Healthc Mater 2018;7. https://doi.org/10.1002/adhm.201700897.
[2] Vig K, Chaudhari A, Tripathi S, Dixit S, Sahu R, Pillai S, et al. Advances in skin regeneration using tissue engineering. Int J Mol Sci 2017;18. https://doi.org/10.3390/ijms18040789.
[3] Goodarzi P, Falahzadeh K, Nematizadeh M, Farazandeh P, Payab M, Larijani B, et al. Tissue engineered skin substitutes. Adv Exp Med Biol. 2018;1107:143–88. https://doi.org/10.1007/5584_2018_226.
[4] Debels H, Hamdi M, Abberton K, Morrison W. Dermal matrices and bioengineered skin substitutes: a critical review of current options. Plast Reconstr Surg Glob Open 2015;3:e284. https://doi.org/10.1097/GOX.0000000000000219.
[5] Dai C, Shih S, Khachemoune A. Skin substitutes for acute and chronic wound healing: an updated review. J Dermatol Treat 2020;31:639–48. https://doi.org/10.1080/09546634.2018.1530443.
[6] Shores JT, Gabriel A, Gupta S. Skin substitutes and alternatives: a review. Adv Skin Wound Care 2007;20:493–508. https://doi.org/10.1097/01.ASW.0000288217.83128.f3.
[7] Li Y, Sawaragi E, Sakamoto M, Nakano T, Yamanaka H, Tsuge I, et al. Development of gelatin hydrogel nonwoven fabrics (Genocel®) as a novel skin substitute in murine skin defects. Regen Ther 2022;21:96–103. https://doi.org/10.1016/j.reth.2022.06.002.
[8] Nakamura K, Saotome T, Shimada N, Matsuno K, Tabata Y. A gelatin hydrogel nonwoven fabric facilitates metabolic activity of multilayered cell sheets. Tissue Eng C Methods 2019;25:344–52. https://doi.org/10.1089/ten.TEC.2019.0061.
[9] Matsuno K, Saotome T, Shimada N, Nakamura K, Tabata Y. Effect of cell seeding methods on the distribution of cells into the gelatin hydrogel nonwoven fabric. Regen Ther 2020;14:160–4. https://doi.org/10.1016/j.reth.2020.01.002.
[10] Nakamura K, Nobutani K, Shimada N, Tabata Y. Gelatin hydrogel-fragmented fibers suppress shrinkage of cell sheet. Tissue Eng C Methods 2020;26:216–24. https://doi.org/10.1089/ten.tec.2019.0348.
[11] Saotome T, Shimada N, Matsuno K, Nakamura K, Tabata Y. Gelatin hydrogel nonwoven fabrics of a cell culture scaffold to formulate 3-dimensional cell constructs. Regen Ther 2021;18:418–29. https://doi.org/10.1016/j.reth.2021.09.008.
[12] Medeiros ES, Glenn GM, Klamczynski AP, Orts WJ, Mattoso LH. Solution blow spinning: a new method to produce micro-and nanofibers from polymer solutions[J]. J Appl Polymer Sci 2009;113(4):2322–30. https://doi.org/10.1002/app.30275.
[13] Pusztaszeri MP, Seelentag W, Bosman FT. Immunohistochemical expression of endothelial markers CD31, CD34, von Willebrand factor, and Fli-1 in normal human tissues. J Histochem Cytochem 2006;54:385–95. https://doi.org/10.1369/jhc.4A6514.2005.
[14] Jamiyan T, Kuroda H, Yamaguchi R, Abe A, Hayashi M. CD68- and CD163-positive tumor-associated macrophages in triple negative cancer of the breast. Virchows Arch 2020;477:767–75. https://doi.org/10.1007/s00428-020-02855-z.
[15] Hwang I, Kim JW, Ylaya K, Chung EJ, Kitano H, Perry C, et al. Tumor-associated macrophage, angiogenesis and lymphangiogenesis markers predict prognosis of non-small cell lung cancer patients. J Transl Med 2020;18:443. https://doi.org/10.1186/s12967-020-02618-z.
[16] Kanda N, Morimoto N, Takemoto S, Ayvazyan AA, Kawai K, Sakamoto Y, et al. Efficacy of novel collagen/gelatin scaffold with sustained release of basic fibroblast growth factor for dermis-like tissue regeneration. Ann Plast Surg 2012;69:569–74. https://doi.org/10.1097/SAP.0b013e318222832f.
[17] Sakamoto M, Morimoto N, Ogino S, Jinno C, Taira T, Suzuki S. Efficacy of gelatin gel sheets in sustaining the release of basic fibroblast growth factor for murine skin defects. J Surg Res 2016;201:378–87. https://doi.org/10.1016/j.jss.2015.11.045.
[18] Li Y, Sakamoto M, Sawaragi E, Nakano T, Katayama Y, Yamanaka H, et al. Comparison of wound healing effect of skin micrograft impregnated into two kinds of artificial dermis in a murine wound model. Plast Reconstr Surgery Glob Open 2022;10:e4636. https://doi.org/10.1097/GOX.0000000000v004636.
[19] Chan BP, Leong KW. Scaffolding in tissue engineering: general approaches and tissue-specific considerations. Eur Spine J 2008;17. https://doi.org/10.1007/s00586-008-0745-3.
[20] Yamamoto M, Takahashi Y, Tabata Y. Controlled release by biodegradable hydrogels enhances the ectopic bone formation of bone morphogenetic protein. Biomaterials 2003;24:4375–83. https://doi.org/10.1016/S0142-9612(03)00337-5.
[21] Ozeki M, Tabata Y. In vivo degradability of hydrogels prepared from different gelatins by various cross-linking methods. J Biomater Sci Polym 2005;16:549–61. https://doi.org/10.1163/1568562053783731.
[22] Kawai K, Suzuki S, Tabata Y, Ikada Y, Nishimura Y. Accelerated tissue regeneration through incorporation of basic fibroblast growth factor-impregnated gelatin microspheres into artificial dermis. Biomaterials 2000;21:489–99. https://doi.org/10.1016/S0142-9612(99)00207-0.
[23] Arif MMA, Fauzi MB, Nordin A, Hiraoka Y, Tabata Y, Yunus MHM. Fabrication of bio-based gelatin sponge for potential use as a functional acellular skin substitute. Polymers 2020;12(11):2678. https://doi.org/10.3390/polym12112678.
[24] Masri S, Maarof M, Mohd NF, Hiraoka Y, Tabata Y, Fauzi MB. Injectable crosslinked genipin hybrid gelatin–PVA hydrogels for future use as bioinks in expediting cutaneous healing capacity: physicochemical characterisation and cytotoxicity evaluation. Biomedicines 2022;10. https://doi.org/10.3390/biomedicines10102651.
[25] Koh TJ, DiPietro LA. Inflammation and wound healing: the role of the macrophage. Expet Rev Mol Med 2011;13:1–12. https://doi.org/10.1017/S1462399411001943.

[26] Hassanshahi A, Moradzad M, Ghalamkari S, Fadaei M, Cowin AJ, Hassanshahi M. Macrophage-mediated inflammation in skin wound healing. Cells 2022;11. https://doi.org/10.3390/cells11192953.
[27] Kotwal GJ, Chien S. Macrophage differentiation in normal and accelerated wound healing. Results Probl Cell Differ 2017;62:353–64. https://doi.org/10.1007/978-3-319-54090-0_14.
[28] Shapouri-Moghaddam A, Mohammadian S, Vazini H, Taghadosi M, Esmaeili SA, Mardani F, et al. Macrophage plasticity, polarization, and function in health and disease. J Cell Physiol 2018;233:6425–40. https://doi.org/10.1002/jcp.26429.
[29] Kloc M, Ghobrial RM, Wosik J, Lewicka A, Lewicki S, Kubiak JZ. Macrophage functions in wound healing. J Tissue Eng Regen Med 2019;13:99–109. https://doi.org/10.1002/term.2772.
[30] Yunna C, Mengru H, Lei W, Weidong C. Macrophage M1/M2 polarization. Eur J Pharmacol 2020;877:173090. https://doi.org/10.1016/j.ejphar.2020.173090.